Groundwater for Sustainable Development 25 (2024) 101131

Contents lists available at ScienceDirect

Groundwater for Sustainable Development

journal homepage: www.elsevier.com/locate/gsd

Research paper

Assessing the impact of climate change on a coastal karst aquifer in a semi-arid area

Marco D'Oria [a,*], Gabriella Balacco [b], Valeria Todaro [a], Maria Rosaria Alfio [b], Maria Giovanna Tanda [a]

[a] Department of Engineering and Architecture, University of Parma, Parco Area delle Scienze, 181/A, 43124, Parma, Italy
[b] Department of Civil, Environmental, Land, Building and Chemical Engineering (DICATECh), Polytechnic University of Bari, Via Orabona, 4, 70125, Bari, Italy

HIGHLIGHTS

- Projections of future groundwater levels in a changing climate.
- Applying simple regression models to link meteorological indices to groundwater levels.
- Adopting a climate model ensemble along with two scenarios to account for uncertainties.

GRAPHICAL ABSTRACT

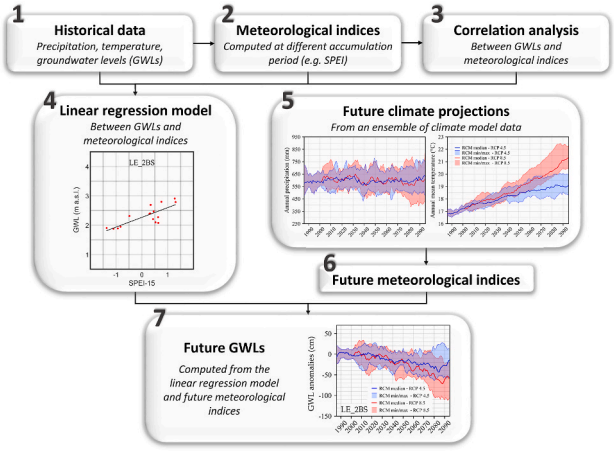

ARTICLE INFO

Keywords:
Climate change
Groundwater levels
Regional climate models
Meteorological indices
Regression modelling

ABSTRACT

This study investigates the potential future state of a coastal karst aquifer located in the Salento peninsula of southern Italy, examining the impact of climate change. After a historical and future overview of the climate in the study area, an analysis of meteorological indices (SPIs and SPEIs) and groundwater levels (GWLs) during the historical period revealed a strong correlation between them. Then, straightforward linear regression models were applied to establish relationships between SPIs/SPEIs and GWLs for the analysed wells. To estimate future SPIs and SPEIs, an ensemble of regional climate models was used, and estimates of GWLs until the end of the century were obtained by incorporating these projections into the regression models. Two emission pathways, the RCP4.5 and the RCP8.5, were considered in the analysis. The results based on SPIs suggest no significant changes in future GWLs across all wells. However, when considering also temperature through the use of SPEIs, a general decline in groundwater levels is expected, with the decrease being more pronounced under the RCP8.5.

* Corresponding author.
E-mail addresses: marco.doria@unipr.it (M. D'Oria), gabriella.balacco@poliba.it (G. Balacco), valeria.todaro@unipr.it (V. Todaro), mariarosaria.alfio@poliba.it (M.R. Alfio), mariagiovanna.tanda@unipr.it (M.G. Tanda).

https://doi.org/10.1016/j.gsd.2024.101131
Received 27 December 2023; Received in revised form 30 January 2024; Accepted 19 February 2024
Available online 20 February 2024

1. Introduction

The rapid changes in climate over the last 150 years cannot be solely attributed to the same natural forces as previous variations. There is evidence that anthropogenic forcing, specifically the release of greenhouse gases, is the main driver of global warming (Caretta et al., 2022). Human activities on Earth have significantly altered the natural water cycle and the Fifth and Sixth Assessment Reports (Jiménez Cisneros and Oki, 2014; IPCC, 2022) of the Intergovernmental Panel on Climate Change (IPCC) showed that climate change is significantly affecting water resources in terms of quantity and quality.

Climate change also affects groundwater systems: directly by influencing replenishment by recharge and indirectly by inducing changes in groundwater use, driven by factors such as land use change and shifts in irrigation demand (Taylor et al., 2013). In particular, the intensification of groundwater extraction has led to a decline in groundwater storage in many places, most notably since the beginning of the 21st century (Caretta et al., 2022). The problem is even more severe in coastal aquifers due to the consequent deterioration of groundwater quality. Increasingly intensive withdrawals contribute to the intrusion of salty water into freshwater aquifers, resulting in saline contamination of water resources (Baena-Ruiz et al., 2020).

Groundwater remains a crucial water resource, mainly for arid regions with limited surface water availability. As climate change intensifies surface water scarcity, the importance of groundwater resources is likely to grow. It is then essential to understand and study the potential effects of climate change on groundwater resources.

Climate models, including Global Circulation Models (GCMs) and Regional Climate Models (RCMs), have the capability to outline potential future climate scenarios (D'Oria et al., 2018a) and enable the identification of near -to long-term climate evolution within a specific area (Pachauri and Meyer, 2014). Consequently, these models play a crucial role in advancing the understanding of how climate change might affect groundwater resources. However, the interactions between climate variables and groundwater resources involve complex dynamics. For instance, the effects of a drought on a groundwater system may take several years to become evident, and different aquifers may respond to changes in hydraulic forcing at varying rates. A complex hydrological/hydrogeological numerical model is often required to comprehend aquifer dynamics thoroughly and assess the potential impact of climate change scenarios on water resources (see e.g., Wu et al., 2020; Arampatzis et al., 2018; Pardo-Igúzquiza et al., 2019; D'Oria et al., 2019; Anurag and Ng, 2022; Sathish et al., 2022; Pulido-Velazquez et al., 2018; Baena-Ruiz et al., 2020). However, set up a comprehensive numerical model of groundwater systems can be challenging. An alternative approach is to investigate direct relationships between climate variables (or meteorological indices derived from them) and groundwater levels (or groundwater indices).

Bloomfield and Marchant (2013) introduced the Standardised Groundwater level Index (SGI) to characterise groundwater droughts. They found a correlation between the SGI and the Standardised Precipitation Index (SPI), with the maximum correlation related to a site-dependent period of precipitation accumulation. The authors also investigated the temporal shift (lag) between SPI and SGI time series to account for the propagation time from climate stimuli to the response of the aquifer system. A linear relationship between the two indices was observed for all sites.

Babre et al. (2022) examined the relationship between the SGI and several meteorological and hydrological drought indices in the Baltic region. The findings indicated that meteorological drought indices, including the SPI, Standardised Precipitation Evapotranspiration Index (SPEI), and Reconnaissance Drought Index (RDI), exhibited the strongest correlation with groundwater conditions. The authors also identified a temporal delay between the climate signal and the response of the aquifer in terms of SGI, analysing correlations at various time lags.

Ndehedehe et al. (2023) conducted a global assessment of spatial correlations between the SPEI and the groundwater surface. They showed positive and negative correlations worldwide, with a preponderance of positive values at the 12-month aggregation scale, suggesting the potential impact of climate change on groundwater. In contrast, negative correlations may be attributed to factors such as extensive withdrawal, complex geological conditions, and aridity.

While various studies have identified potential links between climate variables and groundwater levels, there is a notable lack of research utilizing these relationships to explore future groundwater levels solely based on climate projections (see e.g., Secci et al., 2021; Secci et al., 2023).

This study aims to contribute to this field of research by investigating the potential impacts of climate change on groundwater resources in the Salento area (Apulia region, southern Italy). Currently, the Salento peninsula relies on groundwater as its primary source of freshwater, mainly for drinking and irrigation purposes. This reliance is attributed to the presence of karst geological structures, which facilitate the existence of groundwater resources rather than surface water. A deep understanding of the recharge processes of this aquifer is challenging because of its complex geological and hydrogeological characteristics. Moreover, the limited availability of data makes it difficult to fully comprehend the various phenomena and establish a comprehensive surface/groundwater numerical model, hindering efforts to assess the impact of climate change on groundwater resources. However, despite the complex nature of the aquifer, Balacco et al. (2022a) discovered a direct linkage between meteorological indices, such as SPIs and SPEIs, and groundwater levels (GWLs) collected from different monitoring wells in the Salento area. In this study, projections of GWLs in the short-, medium- and long-term are derived from future projections of SPIs and SPEIs. This is done by assuming straightforward relationships between meteorological indices and GWLs, as observed in the past. SPI and SPEI projections were calculated until the end of this century based on bias-corrected future precipitation and temperature data from an ensemble of RCMs of the EURO-CORDEX initiative (Jacob et al., 2012), under two emission pathways, the RCP4.5 and the RCP8.5.

This paper is structured as follows: Section 2 presents the study area and describes the dataset and methods used; then, the results are presented in Section 3. Section 4 provides a discussion of the main findings and, finally, conclusions are drawn in Section 5.

2. Material and methods

2.1. Study area

The Salento area is a peninsula located in the Apulia region (southern Italy), which covers about 2760 km^2, extending from NW to SE between the Ionian and Adriatic Seas (Fig. 1). The domain is almost flat with few gentle hills in the south. Due to the karst origin, superficial water bodies are practically absent in the area. Intermittent and poorly incised streams sporadically discharge water during intense and heavy rainfall events. The climate of the study area is of Mediterranean type with mild, wet winters and hot, dry summers. The mean annual precipitation (1951–2002) is about 638 mm (Portoghese et al., 2013) and concentrates in the autumn-winter period. The highest temperatures present an average of 25.4 °C for July and August, while the coldest months, January and February, have an average temperature of 9 °C (D'Oria et al., 2018b).

The deep aquifer, whose boundaries coincide with the Salento area, is part of the Apulian carbonate platform, characterised by carbonate rocks of the Jurassic-Cretaceous age. The groundwater circulating within the deep aquifer and floating on marine-origin saltwater serves as the primary source of freshwater for agricultural and drinking purposes in the Salento territory. Additional information about the study area and the geological and hydrogeological context can be found in Alfio et al. (2020), Balacco et al. (2022a) and Parisi et al. (2023).

2.2. Available dataset

2.2.1. Observed data

Precipitation and temperature data from several meteorological stations, along with groundwater level measurements collected in nine monitoring wells, were considered for this study. Continuous groundwater level records were provided by the Geographical Information System of the Apulia Region (http://www.sit.puglia.it/portal/portale_cis/Corpi%20Idrici%20Sotterranei/Dati%20del%20Monitoraggio, accessed on December 6, 2023), after their validation by the Apulia Region - Water Resource Section. The groundwater dataset refers to the Progetto Tiziano, a regional project that ran from July 2007 to December 2011 for the assessment of the qualitative and quantitative status of the Apulian aquifers. Monitoring wells were in static conditions, and monthly levels were calculated from continuous data registered every hour. The piezometric level dataset was complemented with sporadic data (mainly collected during spring and autumn) from 2013 to 2018. The historical climate data were provided by the Civil Protection of the Apulia Government (www.protezionecivile.puglia.it, accessed on December 6, 2023) for thirteen precipitation and nine temperature stations within the Salento area from 1951 to 2020. Monthly precipitation and mean temperature records were available for these stations, although with few gaps within the time series, especially in temperature data. However, Alfio et al. (2023) confirmed that the missing data accounted for less than 7% in daily precipitation and temperature time series over the period 1960–2005, primarily concentrated in the earlier years.

Each monitoring well was paired with a gauging station, resulting in the selection of a total of five precipitation and temperature stations. The selection of the meteorological station most correlated with each monitoring well is supported by the findings of Balacco et al. (2022a), who illustrated that the highest correlation is achieved by opting for the meteorological station closest to the well. Table 1 summarises the main features of the selected wells and the associated meteorological stations, while Fig. 1 shows their locations.

2.2.2. Future climate projections

Precipitation and temperature projections for the Salento area were obtained from an ensemble of 17 climate models of the EURO-CORDEX initiative (https://www.euro-cordex.net, accessed on December 6, 2023). Climate simulations derive from different combinations of GCMs from the CMIP5 long-term experiments and RCMs, as outlined in Table 2. These simulations have a spatial resolution of about 12.5 km (EUR-11 grid). The EURO-CORDEX dataset includes historical experiments that cover the period 1950/1970−2005 and scenario experiments for the period 2006−2098/2100. The historical experiments allow to verify how the RCMs reproduce the characteristics of the past climate and can be used as a reference for comparison with future projections. The future simulations are based on different forcing scenarios. Two Representative Concentration Pathways (RCPs) were considered for this study: the intermediate scenario (RCP4.5) and the most severe scenario (RCP8.5).

RCMs provide the climate data on a regular grid and, for this study, an inverse squared distance method relying on the nine closest grid cells was used to obtain climate projections at the gauging station locations (D'Oria et al., 2017; Todaro et al., 2022). Climate model data are usually

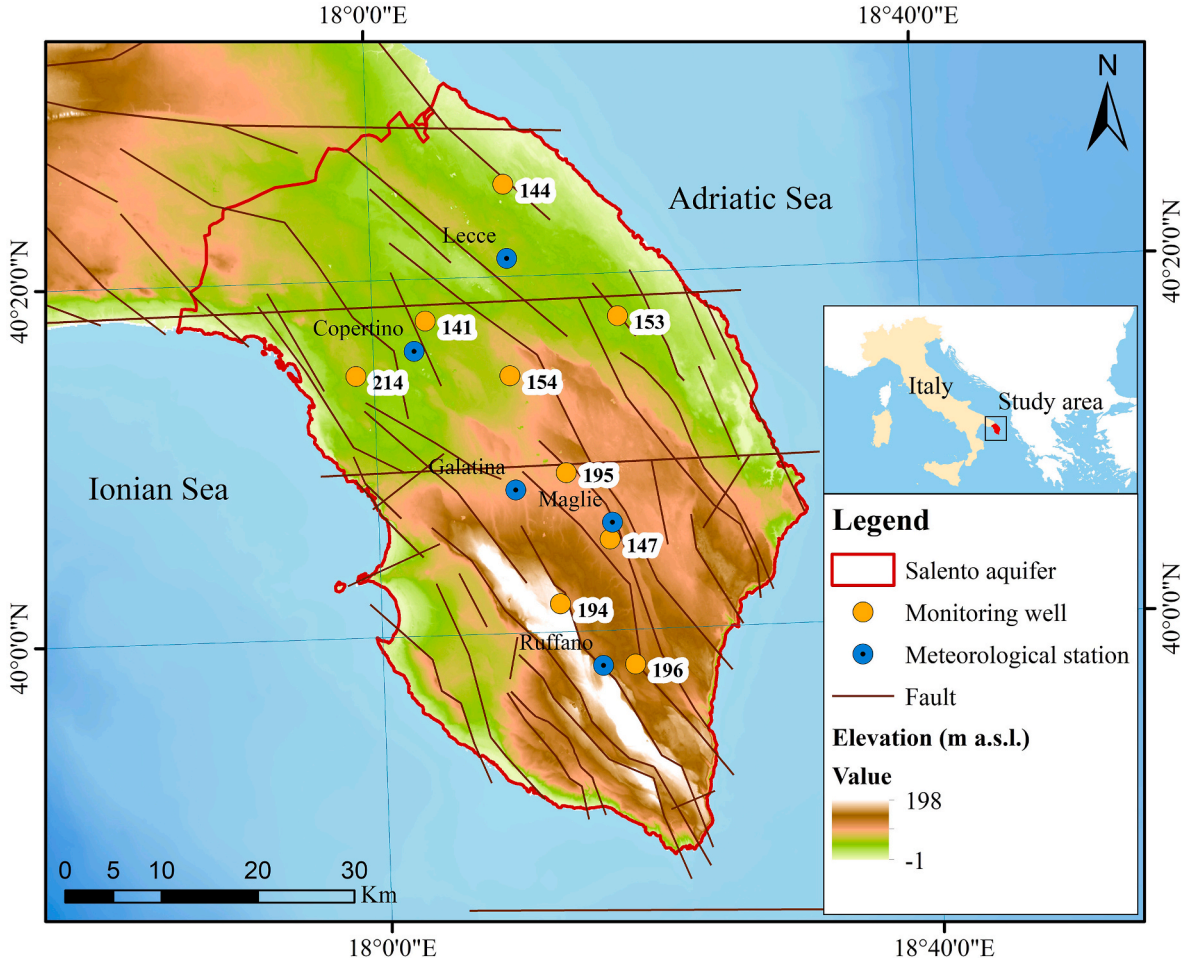

Fig. 1. Study area with locations of monitoring wells and meteorological stations. Wells are assigned a code, as indicated in Table 1.

Table 1
Main features of the selected monitoring wells and meteorological stations.

Well	Code	Lat	Long	Elevation [m a.s.l.]	Well Depth [m]	Station	Lat	Long	Elevation [m a.s.l.]
LE_19/II S	153	40.29	18.30	34.56	227	Lecce	40.35	18.17	51
LE_4/II S	144	40.42	18.17	22.68	100				
LE_12/IIIS	141	40.30	18.07	42.07	62.5	Copertino	40.27	18.05	34
LE_NC4	214	40.25	17.98	48.20	170				
LE_1/LR	154	40.24	18.17	51.41	210				
LE_2/BS	147	40.09	18.28	86.98	113	Maglie	40.10	18.28	102
LE_PS24LE	196	39.97	18.31	106.06	250	Ruffano	39.97	18.26	134
LE_LS21LE	194	40.03	18.22	154.62	230				
LE_PS17LE	195	40.15	18.23	76.69	250	Galatina	40.13	18.16	73

Table 2
GCM-RCM combinations from the EURO-CORDEX initiative.

		GCM					
		CLMcom-CCLM4-8-17	DMI-HIRHAM5	IPSL-INERIS-WRF331F	IPSL-WRF381P	KNMI-RACMO22E	SMHI- RCA4
RCM	CNRM-CERFACS-CNRM-CM5	X				X	X
	ICHEC-EC-EARTH	X	X			X	X
	IPSL-IPSL-CM5A-MR			X	X		X
	MOHC-HadGEM2-ES	X	X			X	X
	MPI-*M*-MPI-ESM-LR	X					X
	NCC-NorESM1-M		X				

affected by systematic errors, requiring bias correction to obtain a dataset that accurately reflects local climate characteristics. Several approaches are available in the literature to perform bias correction of climate model data (see e.g., Teutschbein and Seibert, 2012), which require observations on different time scales (e.g., daily, or monthly records). Since monthly data were used for the study area, a linear-scaling approach was adopted to correct the bias in precipitation and temperature data. Bias correction was conducted for each RCM and gauging station by comparing observed and simulated monthly values during the historical control period 1976–2005. Multiplicative and additive correction factors were applied for precipitation and temperature data, respectively (see D'Oria et al., 2018b for further details). The same correction factors identified in the historical period were used to correct the bias in the scenario period.

2.3. Meteorological drought indices

2.3.1. Standardised Precipitation Index (SPI)

The Standardised Precipitation Index (SPI) is a statistical indicator of wetness or dryness conditions developed by McKee et al. (1993). It requires long monthly precipitation time series, spanning ideally 30 years or more, as the World Meteorological Organization (2012) suggested. Precipitation is usually accumulated over different time scales to account for agricultural droughts (1-3-6 months), hydrological droughts (12 months), and socio-economic impacts (24 months).

The accumulated precipitation is fitted to a suitable probability distribution, in this case, the Gamma distribution, and then transformed into a standard normal distribution. In this study, the SPI time series for the five available stations were computed for the period 1951–2020. To take into account the zero precipitation, a piecewise probability distribution was used:

$$p(x) = \begin{cases} p_0 + (1 - p_0)G(x, \gamma);\ x > 0 \\ p_0 = \dfrac{n_{p=0} + 1}{2(n+1)};\ x = 0 \end{cases} \quad (1)$$

where p is the probability distribution, p_0 is the zero-precipitation probability, $n_{p=0}$ is the number of zero precipitation values in the whole time series, $G(\boldsymbol{x}, \gamma)$ is the Gamma distribution with γ parameters and x is a precipitation element.

Positive SPIs denote wet conditions, whereas negative values refer to dry conditions; according to Mckee et al. (1993), extreme drought occurs when SPI is less than −2.

2.3.2. Standardised Precipitation Evapotranspiration Index (SPEI)

The Standardised Precipitation Evapotranspiration Index (SPEI) was conceptualised by Vicente-Serrano et al. (2010) and Begueria et al. (2013) as a drought index that also accounts for the influence of temperature. It has a similar mathematical structure to SPI, but instead of using precipitation as input, it is based on an accumulated climatic water balance defined as the difference between precipitation and potential evapotranspiration (PET).

For the present work, PET was calculated using the Thornthwaite method (Thornthwaite, 1948) since only mean temperature data were available for the study area.

Unlike the SPI, a log-logistic probability distribution was applied. Following the fitting of the distribution, the data were transformed into a standard normal distribution to derive the SPEI values. The SPEI time series for each station covered the reference period 1951–2020.

2.3.3. SPI and SPEI projections

SPIs and SPEIs were also computed using precipitation and temperature data provided by the 17 climate models in the period 1976–2095. The accumulated precipitation for SPIs and the accumulated difference between precipitation and potential evapotranspiration for SPEIs were transformed into probability values according to the probability distribution functions that fit the observed data in the historical period (1951–2020) and then back-transformed to a standard normal distribution to obtain the meteorological indices.

2.4. Estimation of future groundwater levels

Future groundwater levels were estimated according to straightforward relationships between SPIs and GWLs and between SPEIs and GWLs determined over the historical period in which data for the wells were available (2007–2018). Both the complete dataset and a subset of the data collected during late winter-early spring (specifically in February, March, and April) were analysed. The choice of this subset is motivated by the reduced influence of anthropogenic factors on groundwater conditions during this period. Notably, irrigation

withdrawals are minimal during these months, thus providing a more reliable representation of natural groundwater dynamics.

Each well was coupled with the closest gauging station (Fig. 1 and Table 1), and a correlation analysis was performed, according to the Pearson coefficient, between the recorded GWLs and the meteorological indices evaluated at different accumulation periods (Balacco et al., 2022a). Various time delays (or lags) between meteorological drivers (SPIs and SPEIs) and piezometric levels were also examined to understand the propagation time from the climate to the aquifer system. By considering this delay, it is possible to achieve a better alignment between climate signal and groundwater response, which can result in an improved correlation.

After identifying the time windows and lag-times that exhibited the highest correlation between SPIs and GWLs or between SPEIs and GWLs, a linear regression model was fitted for each well. Under the assumption that the relationships established during the historical period will also apply in the future, the regression models were employed to produce projections of GWLs using the SPIs and SPEIs derived from the climate model data, considering the identified most correlated time windows and lags.

3. Results

3.1. Climate analysis

3.1.1. Precipitation and temperature

A detailed analysis of the climate was conducted for the five gauging stations (Table 2), which were later used to calculate meteorological indices. Monthly precipitation and mean temperature data were available for the selected sites. Based on the observed data presented in Table 3, during the reference period (RP, 1986–2005), the average total annual precipitation ranged from 560 mm (Copertino) to 696 mm (Ruffano). The distribution of precipitation across seasons, not shown for brevity, indicates that autumn accounts for approximately 36% of the total, followed by winter (31%), spring (23%), and summer (10%). Regarding the reference period, the observed annual mean temperature varied from 16.3 °C (Ruffano) to 17.4 °C (Copertino). The highest temperatures were recorded during summer, averaging around 25 °C across all stations, while winter exhibits the coldest temperatures, with an average of 10 °C among the different gauges.

Table 3 also presents the results of the precipitation and temperature analysis obtained from the selected 17 Regional Climate Models (RCMs). The median of the RCM ensemble values for total precipitation well reproduce the observed values during the reference period for all stations, showing deviations ranging from 0.9% to 5.3%. Similarly, the median RCM values closely match the observed annual mean temperature, with a maximum deviation below 0.25 °C. These findings confirm the effectiveness of the bias correction analysis performed in the period 1976–2005.

Having established the reliability of the climate models in replicating historical climate patterns, they were employed to assess future climate conditions at the five selected stations. Two emission pathways, namely RCP4.5 and RCP8.5, were considered for the evaluation.

For the sake of brevity, Fig. 2 shows the projections of the total annual precipitation and annual mean temperature in the period 1986–2095 for the Lecce station. The results are represented in terms of 10-year moving average with the aim of smoothing out natural variability and highlighting the signal of climate change. According to the median values of the climate models, the precipitation time series do not show significant changes in the future. The variability among the RCMs indicates considerable uncertainty in the climate projections. In contrast, temperature projections indicate a progressive warming in the investigated area, especially under the RCP8.5 scenario. The uncertainty associated with temperature data, as represented by the range from minimum to maximum values of the RCMs, tends to amplify over time. The results obtained for the other stations are similar to those of Lecce. Table 3 reports the outcomes of the precipitation and temperature analysis for all gauging stations for three future periods at short- (ST, 2021–2040), medium- (MT, 2041–2060) and long-term (LT, 2076–2095). The changes in twenty-year average annual precipitation and annual mean temperature are calculated as the differences between the ensemble medians of the RCMs of the three future periods and those of the reference period (RP) for temperature, and as percentage variations for precipitation. Table 3 also provides insights into the robustness of the change, indicating a robust change when at least 66% of RCMs (11 out of 17 models) agree in the sign of the change of the RCM ensemble median. For the annual precipitation, positive and negative variations with respect to the reference period were detected; the changes are never robust (with the exception of Ruffano at LT for the RCP8.5), and they are below 5%. When examined on a seasonal scale (results not shown for brevity), the variations exhibit a maximum range of approximately ±25%. Negative values, indicating decreases, are primarily concentrated in the summer and spring seasons, while positive values are concentrated in the winter and autumn seasons. As a result, when analysing the data on an annual scale, the observed variations tend to be relatively small.

On the contrary, temperature changes are always positive and robust, progressively increasing over time. For all stations, the annual mean temperature exhibits an increase of about 0.9 °C in the short-term and up to about 1.9 °C in the long-term for the RCP4.5. For the RCP8.5, the temperature increase ranges from about 1 °C (ST) to approximately 3.6 °C (LT). When analysing the data at a seasonal scale (results not shown), the variations range from 0.8 °C to 2.3 °C for the RCP4.5 and from 0.8 °C to 4.5 °C for the RCP8.5. For a detailed examination of the

Table 3
Observed and RCM median values of the average annual precipitation (mm) and annual mean temperature (°C) for the five gauging stations in the reference period (RP, 1986–2005). Precipitation change (%) and temperature change (°C) between the RCM medians in the short- (ST, 2021–2040), medium- (MT, 2041–2060) and long-term (LT, 2076–2095) and those evaluated in the reference period, for the RCP4.5 and RCP8.5 scenarios. The symbol * denotes a robust change.

				RCP4.5			RCP8.5		
		OBS (mm)	RP (mm)	ST (%)	MT (%)	LT (%)	ST (%)	MT (%)	LT (%)
Precipitation	Copertino	559.7	589.5	−0.8	−2.7	+4.2	+4.9	+0.6	−0.3
	Galatina	661.9	672.3	−3.0	−2.4	+1.1	+4.7	−3.2	+0.1
	Lecce	628.3	633.7	−1.5	−1.8	−1.5	+4.3	−0.5	+0.9
	Maglie	678.7	685.5	−3.1	−3.0	−2.3	+3.7	−3.4	−2.2
	Ruffano	669.5	718.6	−3.2	−3.1	+1.5	+1.2	−1.3	−5.1*
		OBS (°C)	RP (°C)	ST (°C)	MT (°C)	LT (°C)	ST (°C)	MT (°C)	LT (°C)
Temperature	Copertino	17.39	17.31	+0.91*	+1.26*	+1.94*	+1.05*	+1.82*	+3.53*
	Galatina	17.00	16.88	+0.92*	+1.29*	+1.95*	+1.06*	+1.85*	+3.60*
	Lecce	17.25	17.00	+0.92*	+1.26*	+1.95*	+1.04*	+1.83*	+3.56*
	Maglie	16.69	16.57	+0.91*	+1.31*	+1.93*	+1.05*	+1.84*	+3.59*
	Ruffano	16.31	16.07	+0.88*	+1.31*	+1.90*	+1.05*	+1.80*	+3.52*

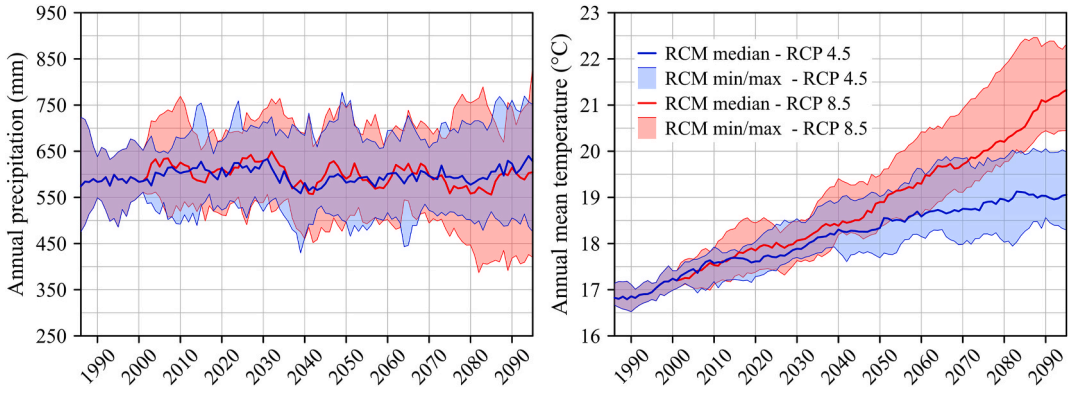

Fig. 2. Annual precipitation (left) and annual mean temperature (right) in terms of 10-year moving average in the period 1986–2095 for the Lecce station under the RCP4.5 and RCP8.5 scenarios. The RCM outputs are shown as the ensemble median (tick line) along with the range encompassing minimum to maximum values (shadow band).

historical and future climate across the study area, refer to D'Oria et al. (2018b) and Alfio et al. (2023).

3.1.2. *Meteorological indices*

SPIs and SPEIs were computed for each gauging station over the period 1951–2020, considering accumulation periods ranging from 1 to 36 months. For the sake of brevity, Fig. 3 shows results only for the Lecce gauging station using time windows of 6, 12, and 24 months, with similar outcomes observed for the other stations. During the analysed period, positive and negative indices alternate. Both SPIs and SPEIs identify the same wet and dry periods, although their specific values may differ. Notably, since the 1980s, there has been an observed increase in the duration of drought periods, accompanied by an increase in the absolute values of the indices. The Lecce gauging station shows an important drought period between 1987 and 1993. Additionally, another significant drought event has been identified in recent years, starting in 2016.

The climate data from the 17 RCMs were utilized to calculate SPIs and SPEIs for the period 1976–2095. To illustrate the potential variations in the meteorological indices in the future, probability density functions (PDFs) were computed for SPIs and SPEIs during the reference period (RP) as well as in the short- (ST), medium- (MT), and long-term (LT), for both the RCP4.5 and RCP8.5. In order to capture the overall tendencies rather than the variability among individual models, the ensemble of climate models was treated as a whole. Consequently, one PDF was generated for each of the selected periods, representing the collective output of the RCM ensemble. For brevity, only the time window of 12 months was analysed in detail. To provide a more comprehensive description and quantification of the changes in the PDFs for all stations, summary statistics such as mode, mean, standard deviation, skewness, and kurtosis are reported in Table 4 for SPIs and Table 5 for SPEIs. As an example, Fig. 4 shows the PDFs for the SPI-12, while Fig. 5 those obtained for the SPEI-12 for the Lecce station. Regarding SPIs, the mean values remain close to zero across the different periods for both the RCP4.5 and the RCP8.5 (Fig. 4 and Table 4). The mode exhibits a similar behaviour, except for the ST period. The standard deviation shows minimal variation for the RCP4.5 but tends to increase for the RCP8.5. With few exceptions, the skewness values generally indicate a right-skewed distribution, where the right tail is longer than the left tail. However, no clear tendency over time is discernible. On the other hand, the kurtosis increases over time (except at LT for the RCP4.5), indicating a transition from a light-tailed distribution (value less than 3) to a heavy-tailed distribution (value greater than 3). This denotes an increase in the probability of extreme SPI values.

The results for SPEIs are quite different. The mean values indicate a progressive leftward shift of the PDFs from RP to LT (Fig. 5 and Table 5),

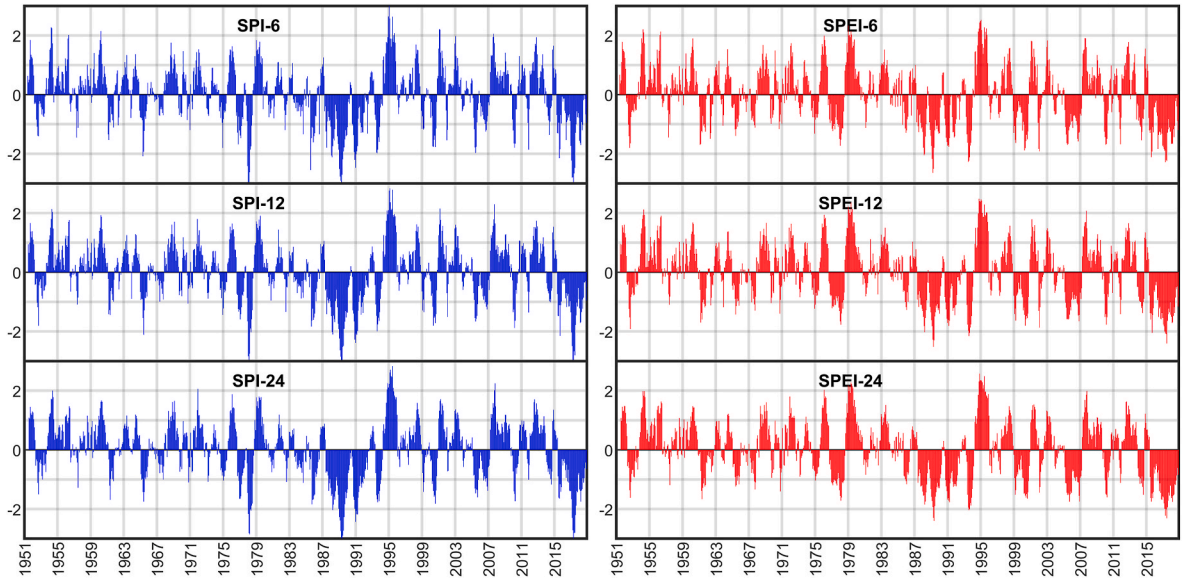

Fig. 3. SPIs (left) and SPEIs (right) evaluated at the accumulation periods of 6, 12 and 24 months for the Lecce gauging station in the historical period 1951–2020.

Table 4
Summary statistics of the SPI-12 time series for the five gauging stations in the reference period (RP, 1986–2005) and in the short- (ST, 2021–2040), medium- (MT, 2041–2060) and long-term (LT, 2076–2095), for the RCP4.5 and RCP8.5 scenarios. The ensemble of climate models was treated as a whole.

			RCP4.5			RCP8.5		
		RP	ST	MT	LT	ST	MT	LT
Copertino	Mode	−0.12	−0.25	−0.24	−0.18	0.12	−0.12	0.13
	Mean	−0.17	−0.13	−0.17	−0.09	−0.02	−0.17	−0.27
	Std	0.78	0.88	0.79	0.91	0.90	0.97	1.09
	Skewness	0.09	−0.07	0.09	0.14	−0.13	0.04	0.09
	Kurtosis	2.84	2.76	3.26	2.82	3.14	3.26	3.28
Galatina	Mode	−0.11	0.00	−0.15	−0.09	0.09	−0.18	0.06
	Mean	−0.13	−0.15	−0.14	−0.09	0.02	−0.19	−0.31
	Std	0.91	1.01	0.95	1.03	1.04	1.12	1.28
	Skewness	0.09	−0.10	0.17	0.14	−0.19	0.15	0.12
	Kurtosis	2.90	2.76	3.26	2.81	3.19	3.46	3.47
Lecce	Mode	−0.18	0.31	−0.01	−0.07	0.38	−0.06	−0.03
	Mean	−0.01	0.02	0.00	0.05	0.12	−0.01	−0.11
	Std	0.75	0.82	0.77	0.86	0.86	0.93	1.04
	Skewness	0.12	−0.03	0.22	0.12	−0.15	0.07	0.12
	Kurtosis	2.89	2.95	3.45	2.80	3.06	3.25	3.50
Maglie	Mode	−0.26	−0.30	−0.36	−0.27	−0.11	−0.41	−0.79
	Mean	−0.22	−0.24	−0.23	−0.22	−0.10	−0.31	−0.42
	Std	0.87	0.99	0.92	0.98	0.99	1.07	1.23
	Skewness	0.09	−0.09	0.25	0.13	−0.16	0.22	0.09
	Kurtosis	2.90	2.85	3.48	2.81	3.14	3.40	3.32
Ruffano	Mode	−0.41	−0.24	0.01	−0.17	0.20	−0.28	−0.13
	Mean	−0.15	−0.18	−0.16	−0.13	−0.02	−0.22	−0.34
	Std	0.89	1.01	0.92	1.01	0.98	1.07	1.25
	Skewness	0.09	−0.11	0.17	0.09	−0.15	0.08	−0.03
	Kurtosis	2.88	2.76	3.21	2.78	3.14	3.01	2.95

Table 5
Summary statistics of the SPEI-12 time series for the five gauging stations in the reference period (RP, 1986–2005) and in the short- (ST, 2021–2040), medium- (MT, 2041–2060) and long-term (LT, 2076–2095), for the RCP4.5 and RCP8.5 scenarios. The ensemble of climate models was treated as a whole.

			RCP4.5			RCP8.5		
		RP	ST	MT	LT	ST	MT	LT
Copertino	Mode	−0.53	−0.99	−1.04	−1.55	−0.69	−1.36	−2.39
	Mean	−0.21	−0.57	−0.86	−1.02	−0.52	−1.02	−1.92
	Std	0.83	0.94	0.82	0.95	0.94	1.01	1.05
	Skewness	0.29	0.32	0.52	0.56	0.33	0.61	0.84
	Kurtosis	2.57	2.80	3.33	2.97	2.88	3.30	4.24
Galatina	Mode	−0.12	−0.79	−0.79	−1.52	−0.40	−1.42	−2.59
	Mean	−0.12	−0.54	−0.77	−1.00	−0.43	−1.02	−2.05
	Std	0.93	1.07	1.00	1.12	1.08	1.18	1.35
	Skewness	0.08	0.06	0.29	0.33	−0.01	0.40	0.54
	Kurtosis	2.50	2.52	2.88	2.62	2.63	2.99	3.24
Lecce	Mode	−0.16	−0.37	−0.75	−1.23	−0.24	−1.12	−2.04
	Mean	0.00	−0.33	−0.56	−0.75	−0.28	−0.74	−1.60
	Std	0.81	0.91	0.84	0.95	0.92	1.01	1.07
	Skewness	0.24	0.21	0.48	0.43	0.18	0.46	0.72
	Kurtosis	2.57	2.74	3.21	2.67	2.70	3.01	3.91
Maglie	Mode	−0.44	−0.79	−0.91	−1.33	−0.69	−1.38	−2.29
	Mean	−0.18	−0.53	−0.73	−0.94	−0.45	−0.95	−1.77
	Std	0.86	0.98	0.90	0.98	0.96	1.05	1.16
	Skewness	0.22	0.22	0.51	0.47	0.18	0.62	0.64
	Kurtosis	2.58	2.66	3.28	2.88	2.66	3.34	3.78
Ruffano	Mode	−0.56	−0.88	−0.94	−0.97	−0.29	−1.22	−2.25
	Mean	−0.13	−0.48	−0.66	−0.85	−0.38	−0.87	−1.67
	Std	0.89	1.02	0.92	1.03	0.98	1.08	1.21
	Skewness	0.20	0.18	0.39	0.40	0.15	0.46	0.45
	Kurtosis	2.57	2.56	3.00	2.80	2.66	2.94	3.26

particularly pronounced in the RCP8.5 scenario. The standard deviation increases over time, suggesting a greater spread of the SPEI values around the mean. The skewness is consistently positive and increases from RP to LT, indicating a progressive deviation of values towards the left side of the mean. Similarly, the kurtosis increases over time, implying a higher concentration of values in the tails.

These patterns are consistent across all stations, indicating that when accounting solely for precipitation (SPIs), minor variations are expected in the future, albeit with a moderate concentration of values in the tails and a slight leftward deviation. However, when incorporating temperature (SPEIs), it becomes evident that the PDFs undergo significant changes over time. They shift towards more negative values, particularly pronounced for the RCP8.5, accompanied by increasing skewness and kurtosis. Based on this analysis, it is expected that groundwater levels will undergo more substantial changes in the future when considering SPEIs compared to SPIs.

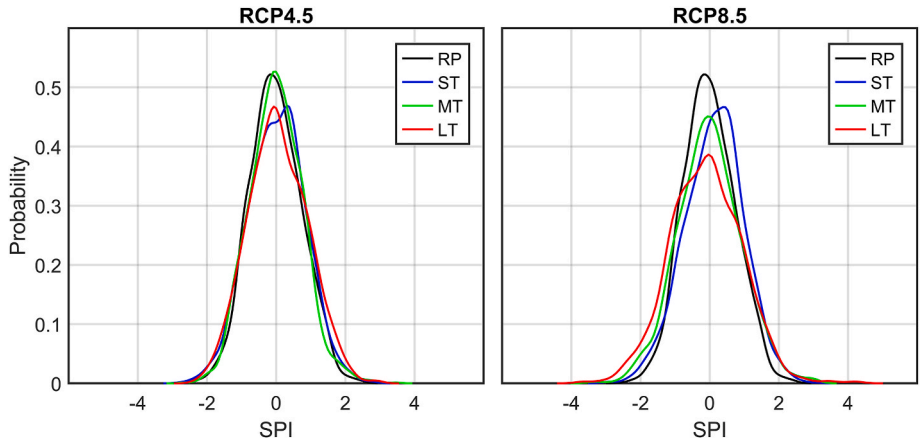

Fig. 4. Probability density function (PDF) of SPI-12 for the Lecce gauging station in the reference period (RP, 1986–2005) and in the short- (ST, 2021–2040), medium- (MT, 2041–2060) and long-term (LT, 2076–2095), for the RCP4.5 and RCP8.5 scenarios. The ensemble of climate models was treated as a whole.

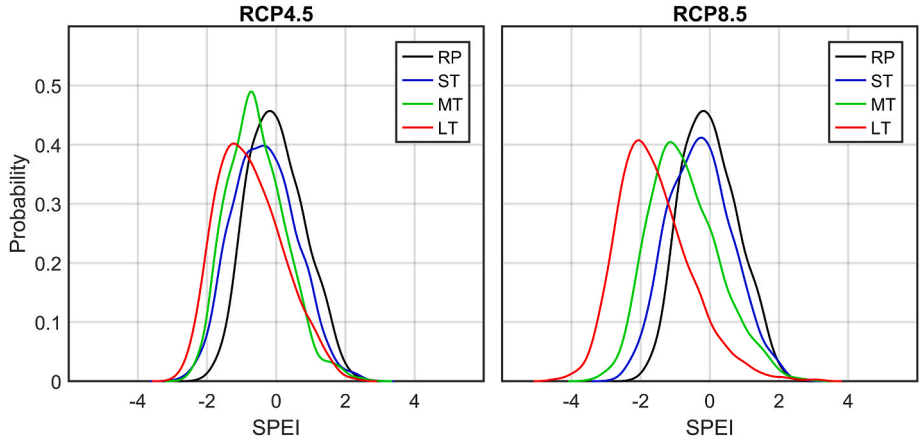

Fig. 5. Probability density function (PDF) of SPEI-12 for the Lecce gauging station in the reference period (RP, 1986–2005) and in the short- (ST, 2021–2040), medium- (MT, 2041–2060) and long-term (LT, 2076–2095), for the RCP4.5 and RCP8.5 scenarios. The ensemble of climate models was treated as a whole.

3.2. Groundwater analysis

3.2.1. Relationships between groundwater levels and meteorological indices

A correlation analysis was performed between GWLs and SPIs and between GWLs and SPEIs computed at several time windows. To consider the time delay in the aquifer system response caused by the propagation time from the climate signal, the correlation between meteorological drivers and GWLs was also investigated for different lags (the lag-time refers to the backward shift of the meteorological indices in relation to the piezometric levels). The historical period 2007–2018 was selected for the analysis since data for the wells were available during that time. Both the complete dataset spanning the entire period and the subset of data collected during late winter-early spring (specifically in February, March, and April) were analysed. Figs. 6 and 7 show the results of the correlation analysis using SPIs and SPEIs, respectively. The findings highlight that the accumulation periods in meteorological indices showing the highest correlations are specific to each well. Taking into account a lag-time can enhance the correlation, leading to improved alignment between meteorological indices and groundwater levels.

While the results are similar for SPI and SPEI analyses, they exhibit notable differences when considering the complete dataset compared to the late winter-early spring subset. Specifically, when analysing the subset, the maximum correlations generally increase (excluding well LE_LR). This can be attributed to the reduced influence of anthropogenic factors during these months (February–April), resulting in a more reliable representation of natural groundwater dynamics. As future groundwater level estimations heavily rely on a robust correlation between groundwater levels and meteorological indices, subsequent analyses will be exclusively based on the late winter-early spring data. Apart from well LE_LR, all wells demonstrate a maximum correlation occurring between 15 and 22 months, accompanied by Pearson correlation coefficients exceeding 0.7 (Table 6 and Table 7), indicating a strong correlation. The lag-times range from 0 to 3 months, indicating a delay between meteorological input and the aquifer response for some wells.

Well LE_LR exhibits very low correlation coefficients (a maximum of 0.36 for both SPI and SPEI) and will be excluded from the further analysis. The findings of Balacco et al. (2022a) also revealed a quite low correlation value for this well. Further investigation at this stage led to the conclusion that this is probably due to the different layout of this borehole, whose extended screen, comprising the transition zone, results in a disturbed groundwater level measurement. Consequently, this measurement may not be representative of the aquifer response.

Once the correlation between SPIs and GWLs and between SPEIs and GWLs was established, linear regression models were developed to link the groundwater levels recorded at the eight remaining monitoring wells with the respective meteorological indices. Figs. 8 and 9 show scatterplots between the GWLs and the corresponding SPIs and SPEIs together with the fitted regression lines. Tables 6 and 7 report the slopes and intercepts of the regression lines for the SPI and SPEI, respectively. Overall, for a given well, there are similarities in the slopes of the regression lines between SPI and SPEI; wells LE_2BS, LE_PS17LE, and LE_LS21LE exhibit the steeper slopes.

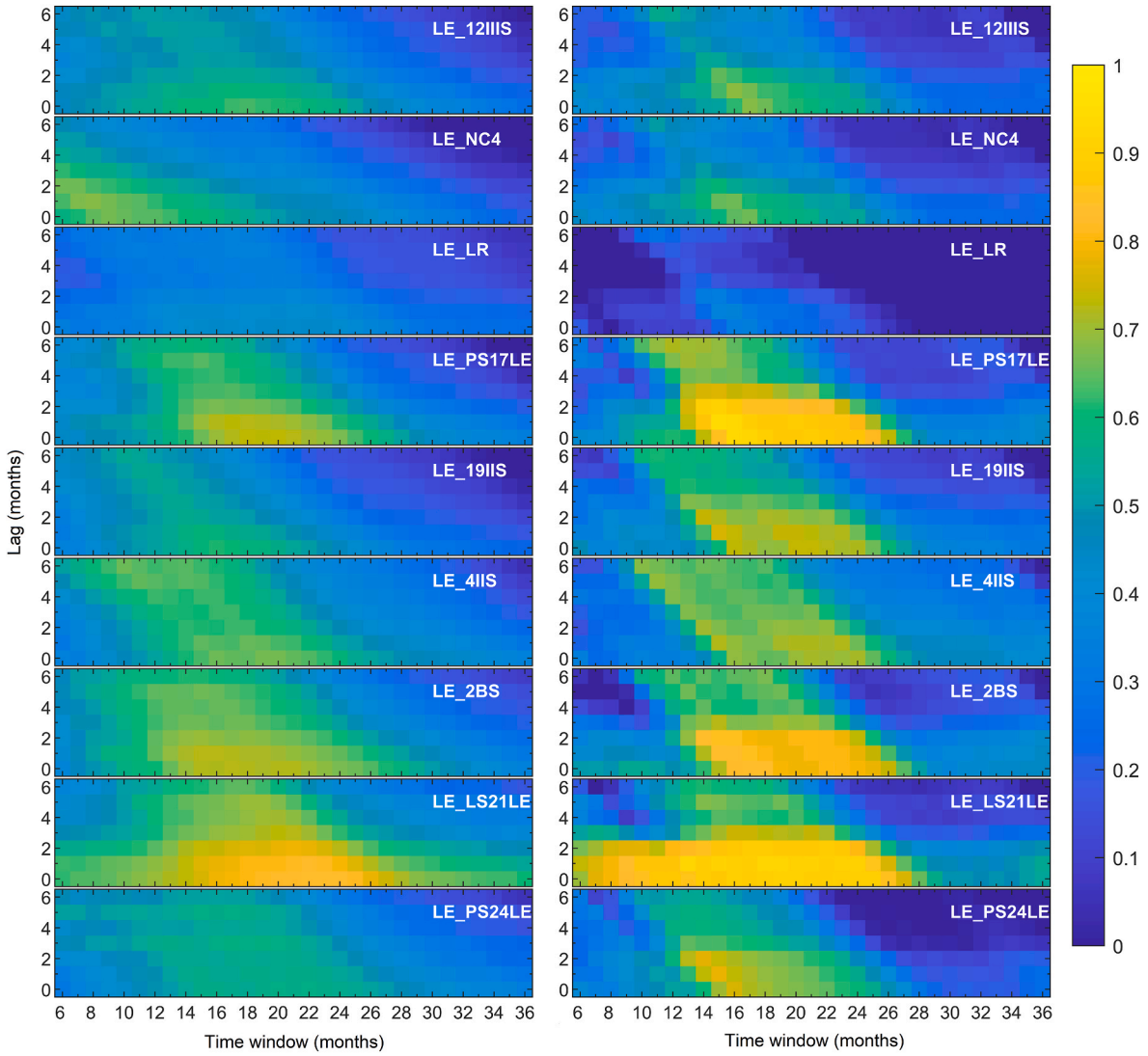

Fig. 6. Heat maps of the Pearson correlation coefficients between GWLs and SPIs for all wells and different time windows and lags. Complete dataset (left), subset of data collected during late winter-early spring (right).

These linear relationships serve as predictive models used to assess the impacts of climate change on the GWLs of the Salento aquifer.

3.2.2. *Future groundwater levels*

Future GWLs were computed based on the linear regression models identified in the historical period in February–April and the future projections of SPIs and SPEIs. Fig. 10 depicts the results for the eight wells in the period 1986–2095 according to the SPI-GWL relationships. The groundwater levels are averaged in the period February–April. To make results between wells comparable, they are represented in terms of GWL anomalies relative to the average GWLs in the reference period, inferred from the RCMs.

According to the RCM ensemble median and both the emission pathways, the analysis indicates that no clear changes in the GWLs are expected in the future for all wells; however, the inter-model variability between the 17 RCMs is different for the eight wells. Wells LE_PS17LE, LE_2BS and LE_LS21LE have the highest uncertainty; the remaining wells show less variability among the RCMs.

To quantify the changes, a trend analysis on the GWL time series over the period 2021–2095 and for both RCP scenarios was conducted. The trends in GWLs were quantified using the Theil-Sen estimator (Sen, 1968) and their presence was determined by means of the Mann-Kendall test (Mann, 1945; Kendall, 1970) at a significance level of 5%. Table 8 reports the number of RCMs that lead to significant positive and negative trends in GWLs and the rate of the changes and its variability, expressed as the mean and standard deviation of the trend gradients obtained from the climate model ensemble, respectively. For the SPI analysis and according to the RCP4.5 scenario, only few RCMs lead to significant positive or negative trends in GWLs for all wells. Overall, the means of the RCM trend gradients highlight negligible changes. According to the RCP8.5 scenario, very few RCMs lead to a significant positive trend and not for all wells; the number of RCMs leading to significant negative trends in GWLs increases, ranging from three to nine depending on the well. The rates of changes are higher than those evaluated with the RCP4.5 but their values still indicate negligible changes; the standard deviations of the trend gradients are comparable with those of the RCP4.5 scenario. The highest mean gradient is expected for the LE_LS21LE well (−3.0 cm/decade).

The future GWL anomalies evaluated using the SPEI-GWL relationships are depicted in Fig. 11. A general decrease in groundwater levels is expected for all wells, which is more severe for the RCP8.5 scenario; the inter-model variability is comparable to that obtained with the SPI analysis. According to the RCP4.5 scenario, the majority of RCMs lead to significant negative trends in GWLs (Table 8), with very few exceptions (at most two RCMs lead to a significant positive trend and only for one well). With the RCP8.5, almost all RCMs point to significant downward

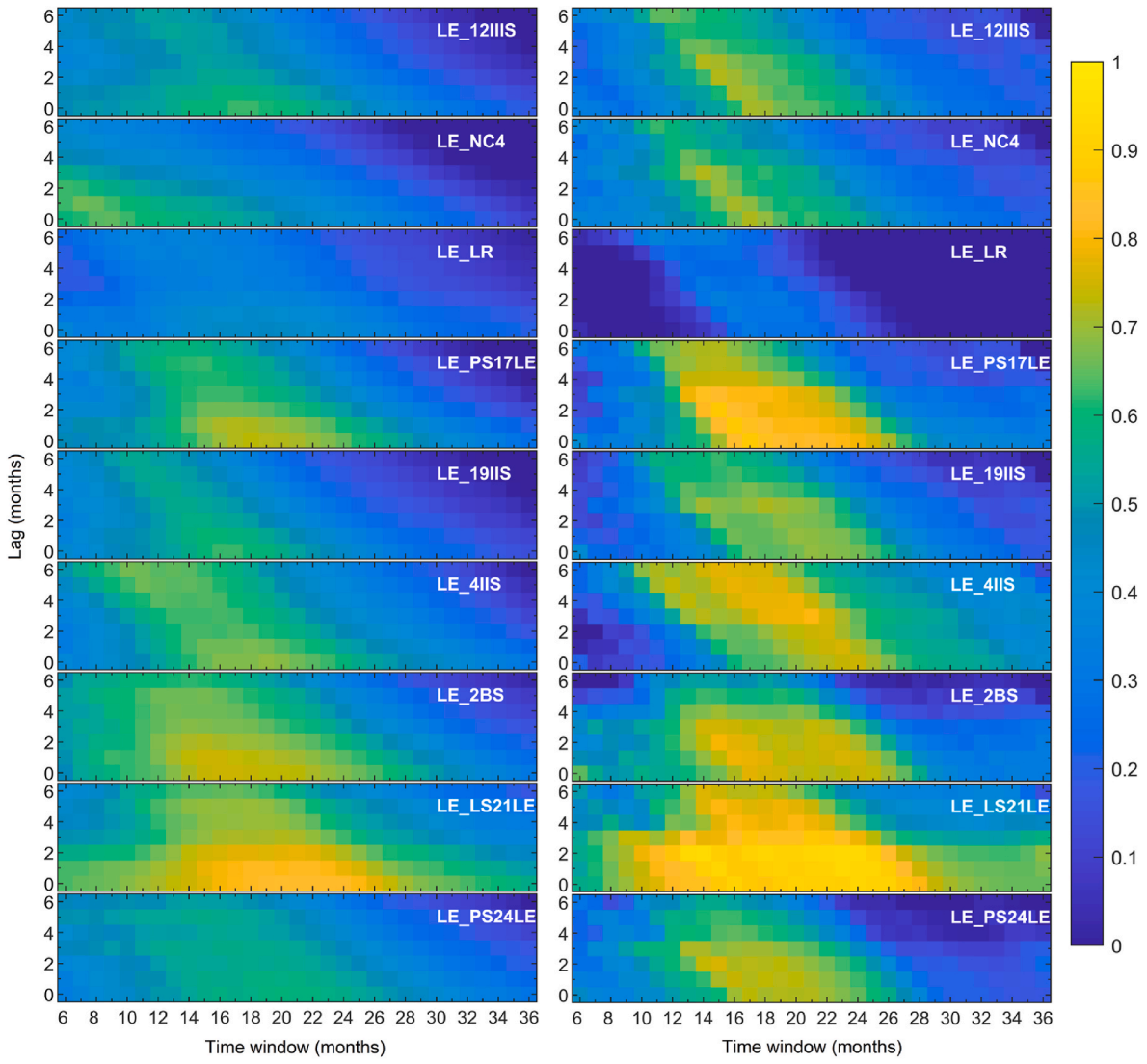

Fig. 7. Heat maps of the Pearson correlation coefficients between GWLs and SPEIs for all wells and different time windows and lags. Complete dataset (left), subset of data collected during late winter-early spring (right).

Table 6
Wells, associated meteorological gauging stations, maximum correlation coefficients between February–April GWLs and SPIs and their accumulation periods and lags in months. Slopes and intercepts (m a.s.l.) of the linear regressions between GWLs and SPIs.

Well	Gauge	Correl.	SPI	Lag	Slope	Interc.
LE_12IIIS	Copertino	0.74	15	2	0.18	1.84
LE_NC4		0.75	14	3	0.10	0.79
LE_LR		0.36	11	6	0.07	2.07
LE_PS17LE	Galatina	0.89	17	0	0.26	2.18
LE_19IIS	Lecce	0.71	18	3	0.13	2.74
LE_4IIS		0.78	21	3	0.12	0.93
LE_2BS	Maglie	0.80	15	2	0.37	2.14
LE_LS21LE	Ruffano	0.95	22	2	0.35	3.53
LE_PS24LE		0.77	15	2	0.19	1.75

Table 7
Wells, associated meteorological gauging stations, maximum correlation coefficients between February–April GWLs and SPEIs and their accumulation periods and lags in months. Slopes and intercepts (m a.s.l.) of the linear regressions between GWLs and SPEIs.

Well	Gauge	Correl.	SPEI	Lag	Slope	Interc.
LE_12IIIS	Copertino	0.72	15	2	0.16	1.88
LE_NC4		0.72	14	3	0.09	0.81
LE_LR		0.36	11	6	0.07	2.09
LE_PS17LE	Galatina	0.88	17	0	0.23	2.26
LE_19IIS	Lecce	0.72	18	3	0.12	2.76
LE_4IIS		0.80	21	3	0.11	0.95
LE_2BS	Maglie	0.80	15	2	0.33	2.27
LE_LS21LE	Ruffano	0.94	14	2	0.44	3.57
LE_PS24LE		0.75	15	2	0.17	1.82

trends of the groundwater levels, regardless of the well. The means of the trend gradients are higher than those computed according to the SPIs, while their standard deviations are comparable, the well being the same. Also in this case, the highest decrease in GWLs is expected for the LE_LS21LE well with a change rate of −3.5 cm/decade for the RCP4.5 and −11.6 cm/decade for the RCP8.5.

Table 9 reports for each well the changes in GWLs in terms of RCM median values between the three future twenty-year periods in the short- (ST), medium- (MT) and long-term (LT) and the reference period (RP). The robustness of the changes, as defined above, is also reported. For the analysis performed using the SPI-GWL relationships, GWL variations are both positive and negative and robust only in a very few cases. According to the RCP8.5, a slight increase in GWLs at ST is expected for all wells; the greatest decreases are found in the LT, but not

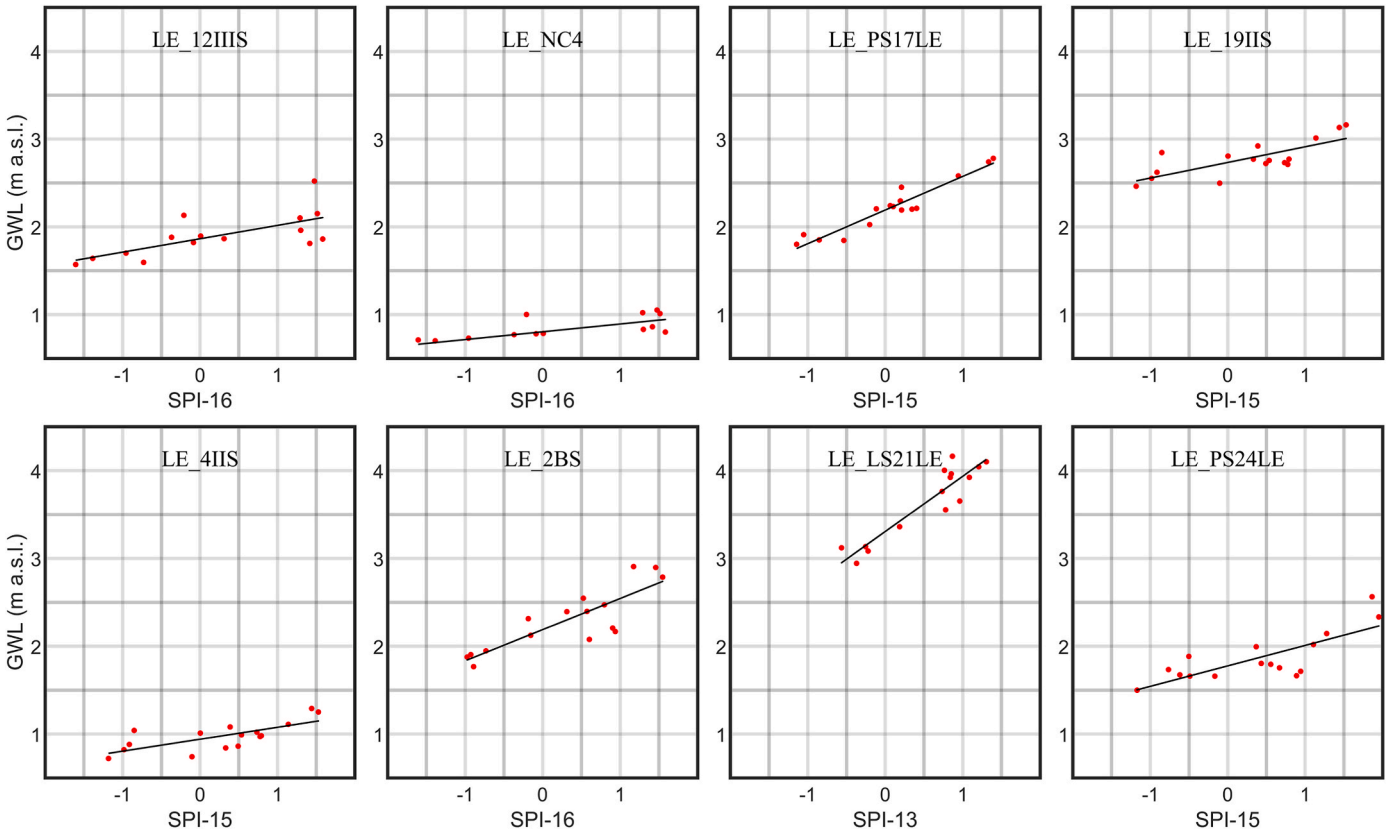

Fig. 8. Scatterplots between February–April GWLs and the corresponding SPIs for the most correlated time window and lag for each well. The regression lines are also reported. The y-scale is the same to allow comparison between groundwater levels within the area and between the slopes of the regression lines.

for all wells. On the contrary, the analysis through the SPEI-GWL relationships leads to robust changes for all wells and scenarios and shows a progressive decrease in the groundwater levels over the investigated area. The highest decreases are expected for the LE_PS17LE, the LE_2BS and the LE_LS21LE wells, which are more sensitive to climate variations as they present the highest slopes of the linear regression models. In particular, for the LE_LS21LE well, GWLs are expected to decrease by 17.3 cm in the short-term up to 38.4 cm in the long-term for the RCP4.5 and up to 72.3 cm (LT) for the RCP8.5.

4. Discussion

A noteworthy topic for discussion pertains to the groundwater system response to the climate signal, which can be inferred from the long-time windows of SPIs and SPEIs and the lag-time that yield the highest correlations with GWLs. Some wells exhibit a delay of up to three months between the climate signal and the groundwater response. This suggests that the climate variables within the delay period have minimal influence on the aquifer response, resulting in a delayed reaction. The extended time windows for the meteorological indices account for the slow dynamics of the aquifer system. Furthermore, the relatively low slope of the regression line for most wells suggests the presence of an attenuation mechanism in the propagation process from meteorological to groundwater droughts (Van Loon, 2015; Secci et al., 2021). This behaviour is also demonstrated by Balacco et al. (2022b) that examined the hydrodynamic characteristics of the Salento aquifer by using time series analyses in the time and frequency domain. Their conclusions highlighted that the system functions as a low-pass filter in response to meteorological events and is characterised by a significant memory effect with high storage capacity.

Beyond climate influences, the response of the groundwater system depends on several factors, mainly local conditions such as geology, surface morphology, permeability of the unsaturated zone, size of the investigated aquifer, withdrawals, and regional flow pattern. The compartmentalization of the aquifer, resulting from its geomorphological and structural characteristics plays a significant role in the local groundwater response of the Salento aquifer (Balacco et al., 2022b). For instance, three wells – LE_2BS, LE_PS17LE and LE_LS21LE – located in close proximity to two faults (Fig. 1) of the same type (i.e., left lateral strike-slip fault with normal component), exhibit the steepest slopes in the linear regression model. This behaviour is likely attributed to the combined effects of recharge from adjacent areas and compartmentalization. All these factors collectively influence the propagation of a meteorological drought to the groundwater (Kumar et al., 2016; Uddameri et al., 2019), introducing a delay between precipitation events and groundwater fluctuations. The regression model employed in this study inherently incorporates many of these influencing factors. In fact, the way in which the groundwater system responds to climate signals, as inferred from the time windows of SPIs and SPEIs along with the lag-time and the slopes of the regression models, is closely linked to the characteristics of the aquifer. Certainly, although the linear regression model is effective in capturing many of these factors, it may not comprehensively encapsulate all the complexities inherent in the groundwater system. This justifies the dispersion of observed points around the regression lines correlating SPIs/SPEIs and GWLs. However, the dispersion tends to be lower for negative SPIs and SPEIs compared to the positive ones, suggesting that the regression model is more reliable during dry periods. This endorses the suggested approach since an essential aspect of water resource management involves the ability to anticipate groundwater droughts.

It is also noteworthy that the monitoring wells exhibit different correlation coefficients between meteorological indices and groundwater levels with each other, which highlights the heterogeneity of the aquifer response. The regression models of those wells that have the

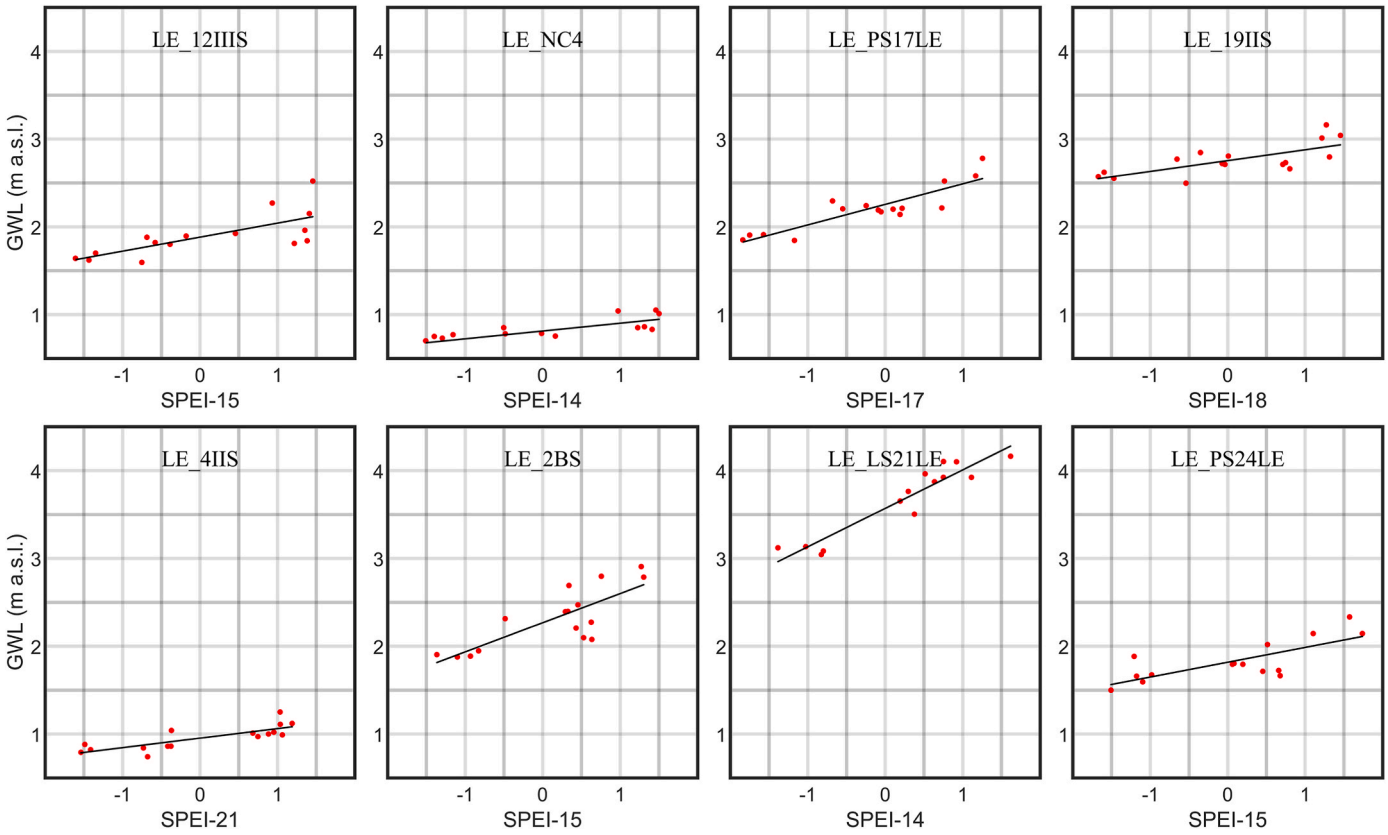

Fig. 9. Scatterplots between February–April GWLs and the corresponding SPEIs for the most correlated time window and lag for each well. The regression lines are also reported. The y-scale is the same to allow comparison between groundwater levels within the area and between the slopes of the regression lines.

highest correlation coefficients would be identified as those with the most reliable results. In this study, three monitoring wells when considering the SPIs and four for the SPEIs showed very strong relationships (Evans, 1996) between meteorological indices and groundwater levels, as indicated by Pearson correlation coefficients between 0.8 and 0.95. Five wells for the SPIs and four for the SPEIs displayed a strong relationship, as indicated by coefficients between 0.71 and 0.78. In the historical period, the correlation between GWLs and both SPIs and SPEIs are similar. Nevertheless, the results of the analysis on the impact of climate change on the groundwater resources differ between the evaluations conducted with SPIs and SPEIs. As mentioned by Vicente-Serrano et al. (2012), the SPI assumes that the variability of precipitation is much higher than that of other variables, such as temperature and potential evapotranspiration (PET). It also assumes that the other variables are stationary without temporal trends. In this context, the SPI primarily considers precipitation as the dominant driver of droughts or wet periods, with the influence of other variables being negligible. In contrast, the SPEI incorporates the influence of temperature as well. In cases where temperature does not exhibit significant trends, such as in the historical period of the study area under consideration, the patterns of SPI and SPEI tend to be similar. However, it is important to note that the role of warming-induced stress on water availability has been increasingly recognized in numerous studies. The anticipated future rise in temperature and its impacts on water resources, according to Vicente-Serrano et al. (2012), suggest the use of the SPEI, especially when the response to drought of the variable of interest is not known a priori. This is particularly relevant in the Salento area, where climate projections indicate that precipitation may not experience significant variations, but the changes will predominantly be driven by an increase in temperature.

Another aspect of discussion is the spread in the results generated by various climate models. A large ensemble of climate models has been chosen for this study, encompassing diverse combinations of GCMs and RCMs, in addition to different emission scenarios. By employing an ensemble approach, it is possible to capture a broader spectrum of potential outcomes and account for the inherent uncertainty in climate projections. Although this uncertainty remains consistent across various gauging stations, it exhibits variability when propagating from climate projections to groundwater levels of the examined wells. In fact, the inter-model variability of groundwater levels is not only due to differences between climate models, but also to the structure of the regression models. The wells that showed low variability among models were those with the smallest slopes in the linear regression models between SPIs or SPEIs and groundwater levels, suggesting that these wells are less sensitive to meteorological variability.

The approach presented in this study relies on a fundamental assumption that the established relationships between groundwater levels and meteorological indices from the historical period will persist in the future. While acknowledging potential limitations, analyzing the historical relationships provides valuable insights into current aquifer dynamics and potential future scenarios. In fact, the historical relationships remain valuable for comprehending existing associations and establishing a baseline understanding. This baseline serves as a reference point for comparing future changes and evaluating the potential impacts of climate change on groundwater resources. One of the key limitations of this study is its inability to incorporate variations in factors, other than climate, that may differ from those observed in the past. Notably, other factors, mainly anthropogenic, could change in the future and affect the availability of groundwater resources. However, predicting future alterations in the human-nature system is challenging, and certain assumptions are necessary when conducting future analyses. In addition, increased pumping volumes or a change in land use, could undoubtedly worsen the impacts on the aquifer. However, the assumptions made regarding the absence of increasing withdrawals and limited

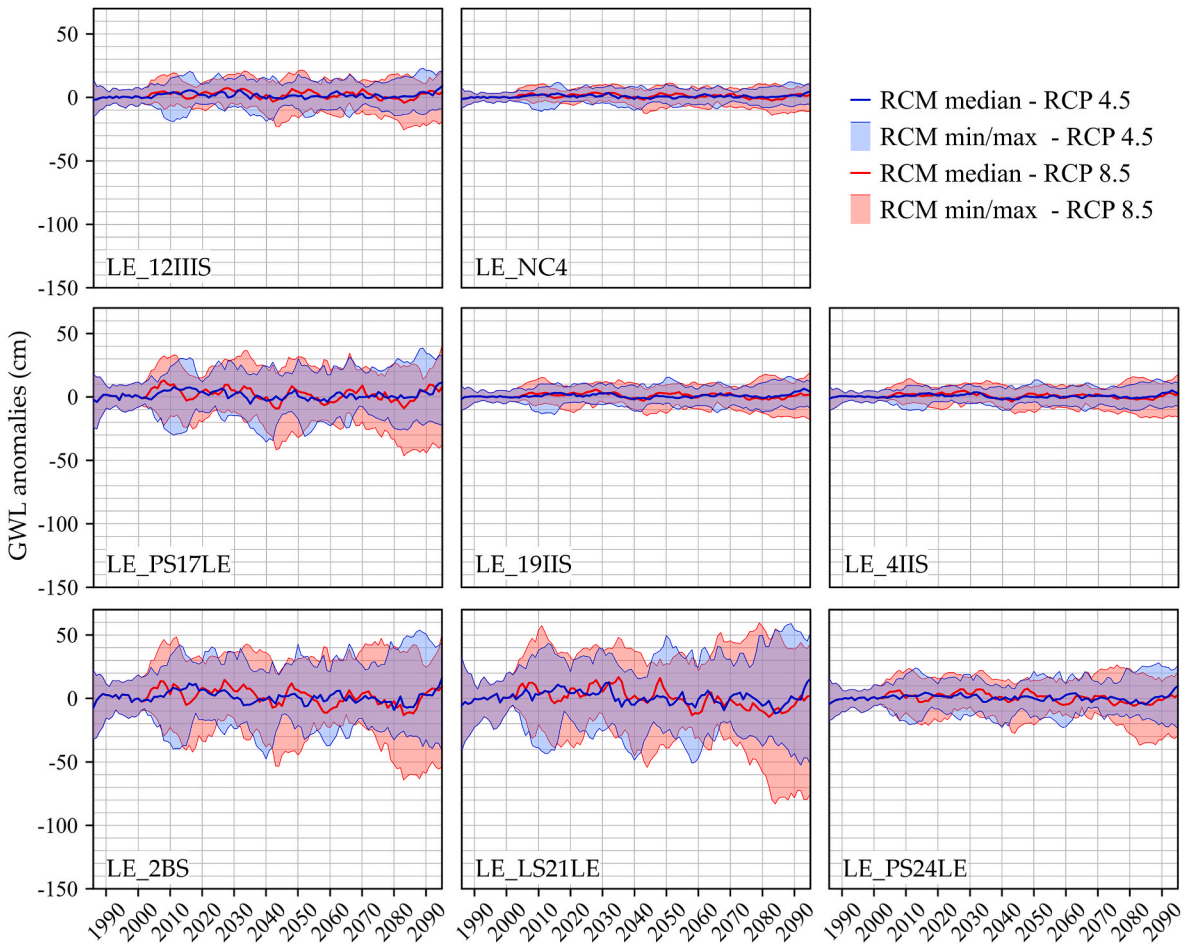

Fig. 10. Groundwater level anomalies, relative to the period 1986–2005, in terms of 10-year moving average for the eight wells according to the SPI-GWL relationships and the RCP4.5 and RCP8.5 scenarios. The results are shown as the ensemble median (tick line) along with the range encompassing minimum to maximum values (shadow band). The GWLs are averaged in the period February–April.

Table 8
February–April groundwater level (according to the SPI-GWL and SPEI-GWL relationships) trend analyses in the period 2021–2095 under the RCP4.5 and RCP8.5 scenarios. #SP and #SN indicate the number of RCMs out of the 17 that leads to positive and negative significant trends (at the 5% significance level), respectively. The mean (cm/decade) and the standard deviation SD (cm/decade) of the trend gradients computed from the RCM ensemble are reported.

		RCP4.5				RCP8.5			
		#SP	#SN	Trend gradient mean	Trend gradient SD	#SP	#SN	Trend gradient mean	Trend gradient SD
SPI	LE_12IIIS	3	0	0.2	1.2	0	5	−0.9	1.4
	LE_NC4	3	0	0.1	0.6	1	3	−0.5	0.7
	LE_PS17LE	3	0	0.2	2.1	0	6	−1.7	2.5
	LE_19IIS	2	0	0.0	0.8	2	5	−0.5	1.1
	LE_4IIS	2	2	0.0	0.8	2	7	−0.6	1.0
	LE_2BS	3	1	0.1	3.0	1	6	−2.3	3.9
	LE_LS21LE	3	4	0.0	3.6	1	9	−3.0	4.7
	LE_PS24LE	4	3	0.1	1.7	0	7	−1.3	2.1
SPEI	LE_12IIIS	0	8	−1.3	1.1	0	16	−4.1	1.3
	LE_NC4	1	9	−0.7	0.6	0	16	−2.4	0.8
	LE_PS17LE	2	9	−2.2	2.0	0	16	−7.6	2.9
	LE_19IIS	0	11	−1.2	0.8	0	16	−3.0	1.1
	LE_4IIS	0	11	−1.1	0.7	0	16	−2.7	0.9
	LE_2BS	1	10	−2.8	2.7	0	15	−8.9	4.1
	LE_LS21LE	1	8	−3.5	3.6	0	14	−11.6	5.3
	LE_PS24LE	1	8	−1.3	1.5	0	14	−4.4	2.1

land use and land cover change for the future appear reasonable for the study area. As per the water resource planning tool (Piano d'Ambito, 2020–2045, https://www.autoritaidrica.puglia.it/aip/po/mostra_news.php?id=6, accessed on December 6, 2023), implemented by the Apulian Water Authority, the approach for addressing water demand in the Apulia region involves expanding the water network and optimizing the use of surface water resources. This strategy has the potential to either maintain or even reduce water withdrawals from the Salento aquifer. Furthermore, Munafò (2022) provide an up-to-date overview of the transformation processes of the Italian land cover, highlighting the

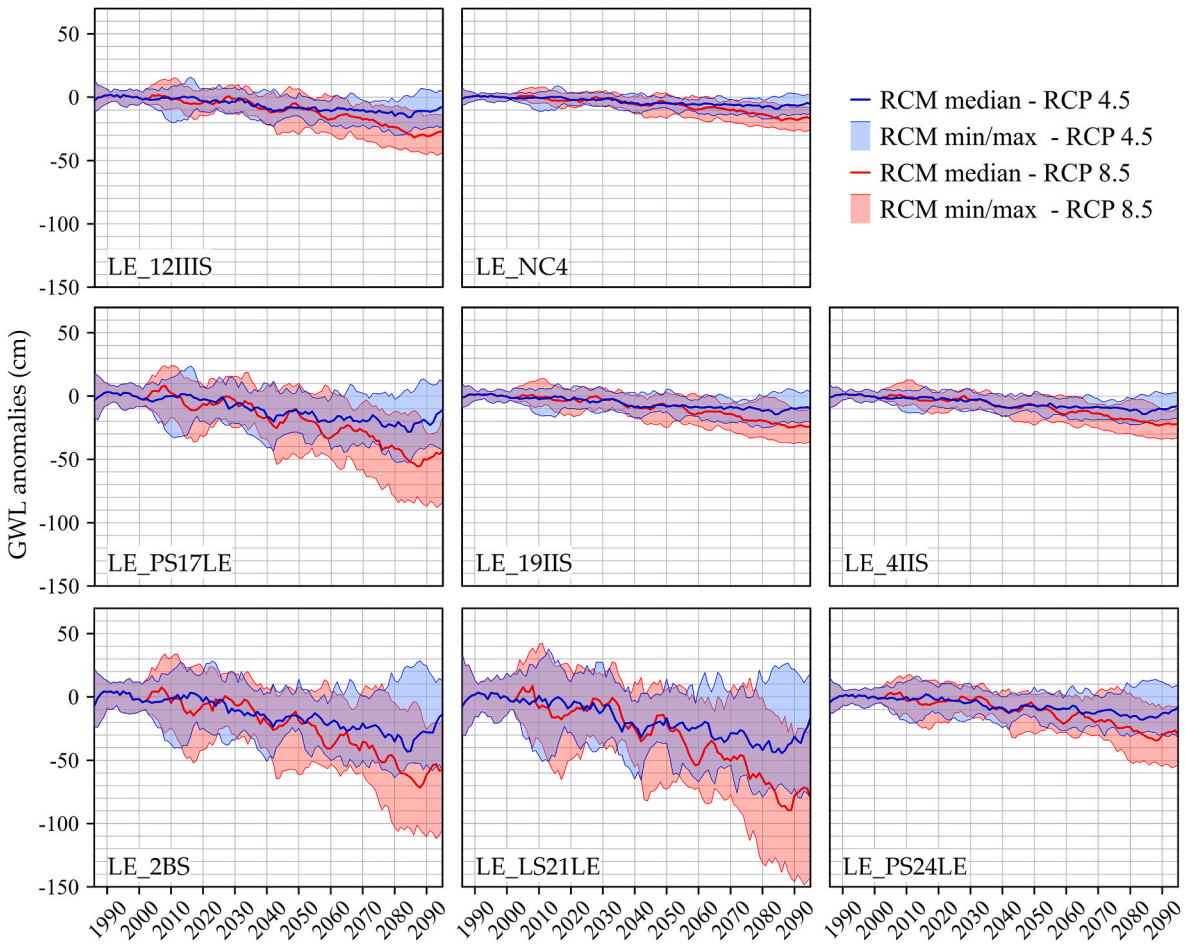

Fig. 11. Groundwater level anomalies, relative to the period 1986–2005, in terms of 10-year moving average for the eight wells according to the SPEI-GWL relationships and the RCP4.5 and RCP8.5 scenarios. The results are shown as the ensemble median (tick line) along with the range encompassing minimum to maximum values (shadow band). The GWLs are averaged in the period February–April.

Salento area as one of the provinces most affected by land consumption (overbuilding, construction of photovoltaic plants and abandonment). This further supports the assumption of neglecting the influence of land use change and the resulting potential increase in water consumption for irrigation purposes.

Another aspect to consider pertains to the availability and quality of the data. The development of a comprehensive model that simulates the mechanisms influencing the availability of groundwater resources is frequently hindered by incomplete information. Thus, obtaining general indications of potential GWL trends, using the approach suggested in this study, proves beneficial in guiding water resource planning, prompting government authorities to take action, and encouraging stakeholders to adopt less water-intensive land uses or, at least, avoid worsening the existing situation.

5. Conclusions

In this work, the potential impacts of climate change on groundwater resources were evaluated by means of historical relationships between meteorological indices and GWLs for monitoring wells located in the Salento aquifer. Future projections of SPIs and SPEIs, estimated using future precipitation and temperature data provided by an ensemble of regional climate models under the climate scenarios RCP4.5 and RCP8.5, were used to evaluate the potential changes in future GWLs.

The understanding of how an aquifer responds to meteorological droughts is crucial for effective water resource management; in this context, meteorological indices can serve as proxy variables to indicate groundwater droughts, which are more challenging to quantify directly. Among the meteorological indices, the SPEI is considered the most suitable index to evaluate the future impact of climate change as it takes both precipitation and temperature into account. For the considered study area, a growing warming is expected, which leads to an increase in drought periods and consequent negative impacts on the groundwater resources, especially under the RCP8.5 scenario.

This study could be of particular interest to regions that are frequently affected by droughts and where groundwater is a crucial resource for their social and economic development. Despite the limitations of regression models in accurately representing complex aquifers, this approach provides a quick and straightforward evaluation of the impact of climate change on aquifers.

Several areas of the Mediterranean depend on the groundwater resources of karst aquifers, where there is a disproportion between aquifer recharge and withdrawals, resulting in a progressive degradation of groundwater quality, particularly pronounced in costal aquifer. This topic is of extreme interest not only for research but also for managing bodies. A future focus will be on the worsening of groundwater quality within aquifers, such as the Salento aquifer, as a result of climate change. An additional future advancement involves incorporating climate models from the CMIP6 experiments. These models were not utilized in the current study because regional climate models, essential for impact studies, are not yet accessible.

Table 9
RCM median values of the February–April GWLs (cm a.s.l.) for the eight wells in the reference period (RP, 1986–2005) computed according to the SPI-GWL and SPEI-GWL relationships. GWL change (cm) between the RCM medians in the short- (ST, 2021–2040), medium- (MT, 2041–2060) and long-term (LT, 2076–2095) and those evaluated in the reference period, for the RCP4.5 and RCP8.5 scenarios. The symbol * denotes a robust change. The colour scale highlights positive (green) and negative (orange) changes.

			RCP4.5			RCP8.5		
		RP	ST	MT	LT	ST	MT	LT
SPI	LE_12IIIS	180.4	1.2*	−0.5	1.9	4.5	1.9	1.1
	LE_NC4	76.8	1.0*	−0.1	0.7	2.7	1.0	0.0
	LE_PS17LE	212.3	−1.9	0.0	2.4	6.7	−4.0	3.9
	LE_19IIS	273.2	0.2	−1.1	0.4	4.0	1.1	0.6
	LE_4IIS	92.2	0.6	−0.7	−0.3	3.3	0.4	−0.5
	LE_2BS	204.7	−4.9	1.4*	−0.7	11.8	−1.9	−0.7
	LE_LS21LE	346.1	−0.2	−2.3	2.9	8.5	−2.4	−4.9*
	LE_PS24LE	172.0	−1.5	−0.3	1.4	4.9	−0.2	−1.1
SPEI	LE_12IIIS	184.1	−4.0*	−9.4*	−10.9*	−2.5*	−10.9*	−28.3*
	LE_NC4	79.3	−2.6*	−5.6*	−6.6*	−1.5*	−6.3*	−16.7*
	LE_PS17LE	220.7	−10.9*	−14.4*	−21.4*	−3.9*	−19.9*	−52.6*
	LE_19IIS	274.8	−4.3*	−7.9*	−10.9*	−2.5*	−9.9*	−22.0*
	LE_4IIS	94.6	−4.2*	−7.5*	−10.5*	−2.7*	−9.8*	−20.6*
	LE_2BS	220.3	−14.1*	−17.8*	−30.2*	−5.1*	−27.5*	−65.2*
	LE_LS21LE	351.0	−17.3*	−20.6*	−38.4*	−9.4*	−32.4*	−72.3*
	LE_PS24LE	179.5	−6.4*	−8.0*	−15.8*	−2.1*	−12.3*	−27.5*

CRediT authorship contribution statement

Marco D'Oria: Writing – review & editing, Writing – original draft, Supervision, Methodology, Conceptualization. **Gabriella Balacco:** Writing – review & editing, Supervision, Methodology, Conceptualization. **Valeria Todaro:** Writing – original draft, Methodology, Formal analysis, Data curation, Conceptualization. **Maria Rosaria Alfio:** Writing – original draft, Methodology, Formal analysis, Data curation, Conceptualization. **Maria Giovanna Tanda:** Writing – review & editing, Supervision, Methodology, Conceptualization.

Declaration of competing interest

The authors declare that they have no known competing financial interests or personal relationships that could have appeared to influence the work reported in this paper.

Data availability

Data will be made available on request.

Acknowledgments

Valeria Todaro acknowledges financial support from PNRR MUR project ECS_00000033_ECOSISTER.

References

Alfio, M.R., Balacco, G., Parisi, A., Totaro, V., Fidelibus, M.D., 2020. Drought index as indicator of salinisation of the Salento aquifer (southern Italy). Water 12, 1927. https://doi.org/10.3390/w12071927.

Alfio, M.R., Pisinaras, V., Panagopoulos, A., Balacco, G., 2023. A comprehensive assessment of RCP4.5 projections and bias-correction techniques in a complex coastal karstic aquifer in the Mediterranean. Front. Earth Sci. 11, 1231296 https://doi.org/10.3389/feart.2023.1231296.

Anurag, H., Ng, G.H.C., 2022. Assessing future climate change impacts on groundwater recharge in Minnesota. J. Hydrol. 612, 128112 https://doi.org/10.1016/j.jhydrol.2022.128112.

Arampatzis, G., Panagopoulos, A., Pisinaras, V., Tziritis, E., Wendland, F., 2018. Identifying potential effects of climate change on the development of water resources in Pinios River Basin, Central Greece. Appl. Water Sci. 8, 51. https://doi.org/10.1007/s13201-018-0690-1.

Babre, A., Kalvāns, A., Avotniece, Z., Retiķe, I., Bikše, J., Popovs, K., Jemeljanova, M., Zelenkevičs, A., Dēliņa, A., 2022. The use of predefined drought indices for the assessment of groundwater drought episodes in the Baltic States over the period 1989–2018. J. Hydrol. Reg. Stud. 40, 101049 https://doi.org/10.1016/j.ejrh.2022.101049.

Baena-Ruiz, L., Pulido-Velazquez, D., Collados-Lara, A.J., Renau-Pruñonosa, A., Morell, I., Senent-Aparicio, J., Llopis-Albert, C., 2020. Summarizing the impacts of future potential global change scenarios on seawater intrusion at the aquifer scale. Environ. Earth Sci. 79, 99. https://doi.org/10.1007/s12665-020-8847-2.

Balacco, G., Alfio, M.R., Fidelibus, M.D., 2022a. Groundwater drought analysis under data scarcity: the case of the Salento aquifer (Italy). Sustainability 14, 707. https://doi.org/10.3390/su14020707.

Balacco, G., Alfio, M.R., Parisi, A., Panagopoulos, A., Fidelibus, M.D., 2022b. Application of short time series analysis for the hydrodynamic characterisation of a coastal karst aquifer: the Salento aquifer (Southern Italy). J. Hydroinf. 24, 420–443. https://doi.org/10.2166/hydro.2022.135.

Beguería, S., Vicente-Serrano, S.M., Reig, F., Latorre, B., 2013. Standardised precipitation evapotranspiration index (SPEI) revisited: parameter fitting, evapotranspiration models, tools, datasets and drought monitoring. Int. J. Climatol. 34, 3001–3023. https://doi.org/10.1002/joc.3887.

Bloomfield, J.P., Marchant, B.P., 2013. Analysis of groundwater drought building on the standardised precipitation index approach. Hydrol. Earth Syst. Sci. 17, 4769–4787. https://doi.org/10.5194/hess-17-4769-2013.

Caretta, M.A., Mukherji, A., 2022. Water. In: Portner, H.-O., Roberts, D.C., Tignor, M., Poloczanska, E.S., Mintenbeck, K., Alegría, A., Craig, M., Langsdorf, S., Loschke, S., Moller, V., Okem, A., Rama, B. (Eds.), Climate Change 2022: Impacts, Adaptation and Vulnerability. Contribution of Working Group II to the Sixth Assessment Report of the Intergovernmental Panel on Climate Change. Cambridge University Press, Cambridge, UK and New York, NY, USA, pp. 551–712. https://doi.org/10.1017/9781009325844.006.

D'Oria, M., Ferraresi, M., Tanda, M.G., 2017. Historical trends and high-resolution future climate projections in northern tuscany (Italy). J. Hydrol. 555, 708–723. https://doi.org/10.1016/j.jhydrol.2017.10.054.

D'Oria, M., Cozzi, C., Tanda, M.G., 2018a. Future precipitation and temperature changes over the taro, parma and enza river basins in northern Italy. Ital. J. Eng. Geol. Environ. 49–63. https://doi.org/10.4408/IJEGE.2018-01.S-05.

D'Oria, M., Tanda, M.G., Todaro, V., 2018b. Assessment of local climate change: historical trends and RCM multi-model projections over the Salento area (Italy). Water 10, 978. https://doi.org/10.3390/w10080978.

D'Oria, M., Ferraresi, M., Tanda, M.G., 2019. Quantifying the impacts of climate change on water resources in northern Tuscany, Italy, using high-resolution regional projections. Hydrol. Process. 33, 978–993. https://doi.org/10.1002/hyp.13378.

Evans, J.D., 1996. Straightforward Statistics for the Behavioral Sciences, Pacific Gr. Pacific Grove. Brooks/Cole Publishing, , CA.

IPCC, 2022. Climate Change 2022: Impacts, Adaptation and Vulnerability, Summary for Policymakers. Cambridge University Press, Cambridge, UK and New York, USA.
Jacob, D., Elizalde, A., Haensler, A., Hagemann, S., Kumar, P., Podzun, R., Rechid, D., Remedio, A.R., Saeed, F., Sieck, K., Teichmann, C., Wilhelm, C., 2012. Assessing the transferability of the regional climate model REMO to different coordinated regional climate downscaling experiment (CORDEX) regions. Atmosphere 3, 181–199. https://doi.org/10.3390/atmos3010181.
Jiménez Cisneros, B.E., Oki, T., 2014. Freshwater resources. In: Field, C.B., Barros, V.R., Dokken, D.J., Mach, K.J., Mastrandrea, M.D., Bilir, T.E., Chatterjee, M., Ebi, K.L., Estrada, Y.O., Genova, R.C., Girma, B., Kissel, E.S., Levy, A.N., MacCracken, S., Mastrandrea, P.R., White, L.L. (Eds.), Climate Change 2014: Impacts, Adaptation, and Vulnerability. Part A: Global and Sectoral Aspects. Contribution of Working Group II to the Fifth Assessment Report of the Intergovernmental Panel of Climate Change. Cambridge University Press, Cambridge, United Kingdom and New York, NY, USA, pp. 229–269.
Kendall, M.G., 1970. Rank Correlation Methods, fourth ed. Griffin, London, UK. ISBN 9780852641996.
Kumar, R., Musuuza, J.L., Van Loon, A.F., Teuling, A.J., Barthel, R., Ten Broek, J., Mai, J., Samaniego, L., Attinger, S., 2016. Multiscale evaluation of the Standardised Precipitation Index as a groundwater drought indicator. Hydrol. Earth Syst. Sci. 20, 1117–1131. https://doi.org/10.5194/hess-20-1117-2016.
Mann, H.B., 1945. Nonparametric tests against trend. Econometrica 13, 245.
Mckee, T.B., Doesken, N.J., Kleist, J., 1993. The relationship of drought frequency and duration to time scales. In: Proceedings of the Eight Conference on Applied Climatology, 17–22 January 1993 Anaheim. CA, USA.
Munafò, M., 2022. Consumo di suolo, dinamiche territoriali e servizi ecosistemici. Edizione 2022. Report SNPA (in Italian).
Ndehedehe, C.E., Ferreira, V.G., Adeyeri, O.E., Correa, F.M., Usman, M., Oussou, F.E., Kalu, I., Okwuashi, O., Onojeghuo, O., Getirana, A., 2023. Global assessment of drought characteristics in the Anthropocene. Resour. Environ. Sustain. 12, 100105 https://doi.org/10.1016/j.resenv.2022.100105.
Pachauri, R.K., Meyer, L.A., 2014. Climate Change 2014: Synthesis Report. Contribution of Working Groups I, II and III to the Fifth Assessment Report of the Intergovernmental Panel on Climate Change. IPCC, Geneva, Switzerland.
Pardo-Igúzquiza, E., Collados-Lara, A.J., Pulido-Velazquez, D., 2019. Potential future impact of climate change on recharge in the Sierra de las Nieves (southern Spain) high-relief karst aquifer using regional climate models and statistical corrections. Environ. Earth Sci. 78, 598. https://doi.org/10.1007/s12665-019-8594-4.
Parisi, A., Alfio, M.R., Balacco, G., Güler, C., Fidelibus, M.D., 2023. Analyzing spatial and temporal evolution of groundwater salinisation through multivariate statistical analysis and hydrogeochemical facies evolution-diagram. Sci. Total Environ. 862, 160697 https://doi.org/10.1016/j.scitotenv.2022.160697.
Portoghese, I., Bruno, E., Dumas, P., Guyennon, N., Hallegatte, S., Hourcade, J.C., Nassopoulos, H., Pisacane, G., Struglia, M.V., Vurro, M., 2013. Impacts of climate change on freshwater bodies: quantitative aspects. Adv. Glob. Change Res. 50, 241–304. https://doi.org/10.1007/978-94-007-5781-3_9.
Pulido-Velazquez, D., Renau-Pruñonosa, A., Llopis-Albert, C., Morell, I., Collados-Lara, A.J., Senent-Aparicio, J., Baena-Ruiz, L., 2018. Integrated assessment of future potential global change scenarios and their hydrological impacts in coastal aquifers - a new tool to analyse management alternatives in the Plana Oropesa-Torreblanca aquifer. Hydrol. Earth Syst. Sci. 22, 3053–3074. https://doi.org/10.5194/hess-22-3053-2018.
Sathish, S., Chanu, S., Sadath, R., Elango, L., 2022. Impacts of regional climate model projected rainfall, sea level rise, and urbanisation on a coastal aquifer. Environ. Sci. Pollut. Res. 29, 33305–33322. https://doi.org/10.1007/s11356-021-18213-8.
Secci, D., Tanda, M.G., D'Oria, M., Todaro, V., Fagandini, C., 2021. Impacts of climate change on groundwater droughts by means of standardised indices and regional climate models. J. Hydrol. 603, 127154 https://doi.org/10.1016/j.jhydrol.2021.127154.
Secci, D., Tanda, M.G., D'Oria, M., Todaro, V., 2023. Artificial intelligence models to evaluate the impact of climate change on groundwater resources. J. Hydrol. 627, 130359 https://doi.org/10.1016/j.jhydrol.2023.130359.
Sen, P.K., 1968. Estimates of the regression coefficient based on kendall's tau. J. Am. Stat. Assoc. 63, 1379–1389.
Taylor, R.G., Scanlon, B., Döll, P., Rodell, M., van Beek, R., Wada, Y., Longuevergne, L., Leblanc, M., Famiglietti, J.S., Edmunds, M., Konikow, L., Green, T.R., Chen, J., Taniguchi, M., Bierkens, M.F.P., MacDonald, A., Fan, Y., Maxwell, R.M., Yechieli, Y., Gurdak, J.J., Allen, D.M., Shamsudduha, M., Hiscock, K., Yeh, P.-F., Holman, I., Treidel, H., 2013. Ground water and climate change. Nat. Clim. Change 3, 322–329. https://doi.org/10.1038/nclimate1744.
Teutschbein, C., Seibert, J., 2012. Bias correction of regional climate model simulations for hydrological climate-change impact studies: review and evaluation of different methods. J. Hydrol. 456–457, 12–29. https://doi.org/10.1016/j.jhydrol.2012.05.052.
Thornthwaite, C.W., 1948. An approach toward a rational classification of climate. Geogr. Rev. 38, 55. https://doi.org/10.2307/210739.
Todaro, V., D'Oria, M., Secci, D., Zanini, A., Tanda, M.G., 2022. Climate change over the mediterranean region: local temperature and precipitation variations at five pilot sites. Water 14, 2499. https://doi.org/10.3390/w14162499.
Uddameri, V., Singaraju, S., Hernandez, E.A., 2019. Is standardised precipitation index (SPI) a useful indicator to forecast groundwater droughts? — Insights from a karst aquifer. J. Am. Water Resour. Assoc. 55, 70–88. https://doi.org/10.1111/1752-1688.12698.
Van Loon, A.F., 2015. Hydrological drought explained. WIREs Water 2, 359–392. https://doi.org/10.1002/wat2.1085.
Vicente-Serrano, S.M., Beguería, S., López-Moreno, J.I., 2010. A multiscalar drought index sensitive to global warming: the standardised precipitation evapotranspiration index. J. Clim. 23, 1696–1718. https://doi.org/10.1175/2009JCLI2909.1.
Vicente-Serrano, S.M., Beguería, S., Lorenzo-Lacruz, J., Camarero, J.J., López-Moreno, J.I., Azorin-Molina, C., Revuelto, J., Morán-Tejeda, E., Sanchez-Lorenzo, A., 2012. Performance of drought indices for ecological, agricultural, and hydrological applications. Earth Interact. 16, 1–27. https://doi.org/10.1175/2012EI000434.1.
World Meteorological Organization, 2012. Standardized Precipitation Index User Guide. WMO-No. 1090, Geneva, Switzerland.
Wu, W.Y., Lo, M.H., Wada, Y., Famiglietti, J.S., Reager, J.T., Yeh, P.J.F., Ducharne, A., Yang, Z.L., 2020. Divergent effects of climate change on future groundwater availability in key mid-latitude aquifers. Nat. Commun. 11, 3710. https://doi.org/10.1038/s41467-020-17581-y.